Carbon-enriched coal fly ash as a precursor of activated carbons for SO₂ removal

M.T. Izquierdo, B. Rubio *

Instituto de Carboquímica (CSIC), Miguel Luesma Castán 4, 50018-Zaragoza, Spain

Abstract

Carbon-enriched coal fly ash was evaluated in this work as a low-cost adsorbent for SO_2 removal from stack gases. The unburned carbon in coal fly ash was concentrated by mechanical sieving and vegetal oil agglomeration. The carbon concentrates were activated with steam at 900 °C in order to develop porosity onto the samples. The performance of these samples in the SO_2 abatement was tested in the following conditions: 100 °C, 1000 ppmv SO_2, 5% O_2, 6% water vapor. A good SO_2 removal capacity was shown by some of the studied samples that can be related to their textural properties. Cycles of SO_2 adsorption/regeneration were carried out in order to evaluate the possibility of thermal regeneration and re-use of these carbons. Regeneration of the exhausted carbons was carried out at 400 °C of temperature and a flow of 25 ml/min of Ar. After each cycle, the SO_2 removal capacity of the sample decreases.
© 2007 Elsevier B.V. All rights reserved.

Keywords: Carbon-enriched coal fly ash; Vegetal oil agglomeration; Activated carbon; SO₂ removal

1. Introduction

The fly ash (FA) produced from the burning of pulverized coal in a coal-fired boiler is a fine-grained, powdery particulate material that is carried off in the flue gas and usually collected from the flue gas by means of electrostatic precipitators, baghouses, or mechanical collection devices such as cyclones.

When pulverized coal is combusted in a dry-ash, dry-bottom boiler, about 80% of all the ash leaves the furnace as fly ash. Approximately 45 million tonnes were produced in 2005 in the EU15 [1]. Within the EU, the utilization for FA in the construction industry is currently around 47%, about 42% are used as a replacement for naturally occurring resources and the rest is disposed.

FAs consist mainly of oxides of silica, aluminum, iron and calcium. Some unburnt or partially unburnt carbon residue is collected with the FA in the precipitators [2]. Reduction of NO*x* emissions through the installation of low NO*x* burners often results in higher unburned carbon contents in the FA, decreasing the marketability of some ashes. Unburned carbon tends to

adsorb the air-entrainment reagents that are added to the cement to prevent crack formation and propagation.

The fate of this unburned carbon is mainly disposal due to the present lack of routes for their effective use. In recent years, unburned carbon has been explored as low cost adsorbents replacing activated carbon for flue gas treatment. The carbon present in FAs can be a precursor of activated carbons since it has gone through a devolatilization during the combustion in the furnace of the power station and, therefore, it only requires a process of activation [3,4].

Unburned carbon has been tested as an adsorbent for the treatment of wastewater from dyeing [5,6], mercury adsorption [7,8] and also as catalyst in low temperature NO reduction with ammonia [9].

An application few explored until the present of the activated carbons obtained from carbon-enriched fly ash is the SO_2 removal from stack gas.

The removal of SO_2 over a carbon in the presence of oxygen and water vapor at low temperature involves a series of reactions that leads to the formation of sulfuric acid as the final product. The role of a carbon material is to allow the adsorption of SO_2, H_2O and O_2 at the internal surface of the carbon, the catalytic oxidation of adsorbed SO_2 to sulfuric acid and storage of the generated acid in the pores [10].

* Corresponding author. Tel.: +34 976 733977; fax: +34 976 733318.
E-mail address: brubio@icb.csic.es (B. Rubio).

The aim of this investigation was to evaluate the SO_2 abatement capacity of activated carbons obtained from fly ash carbon-rich fractions activated with steam.

2. Materials and methods

2.1. Samples preparation

Coal fly ash (FA) from a pulverized coal power plant in Spain (Escucha, Teruel) was chosen as a starting material (named E2) to obtain an enriched carbon fraction. Approximately 50 kg of FA were sieved into different mesh fractions in order to select the fraction richer in carbon. The characterization of the sieved fractions [11] leaded to select a cut of particle size bigger than 200 μm to obtain carbon-enriched sample E2-EN.

This sample enriched in unburned carbon was agglomerated with vegetable oil according to a procedure described elsewhere [12]. Oil agglomeration was conducted in a commercial blender equipped with a 1000 ml glass vessel. Approximately 16 g of sample and 400 ml of distilled water were placed in the blender and mixed at 11,000 rpm for 5 min to disperse the particles. After this an amount corresponding to 2 wt% of sample was added and mixing was continued at same speed for 1 min to produce agglomerates. The resultant agglomeration product was separated from the refuse by froth flotation in a flotation machine using air. The agglomerates were filtered, washed with ethanol, perchloroethylene and ethyl ether to extract the oil, water-washed and dried. A part of sample E2-EN-AG was heated in Ar at 550 °C in order to remove any residual oil. The resulting sample was named E2-EN-AG-550.

Both types of samples, sieving-enriched and oil-agglomerated, were activated with steam in a fluidized bed, in a flow containing 95% water vapor and 5% nitrogen, at 900 °C during 2 h. After this period of time, the flow of water vapor was cut off and a flow of nitrogen is passed through the bed until the sample is cooled down. Activated samples were named E2-EN-ACT and E2-EN-AG-ACT.
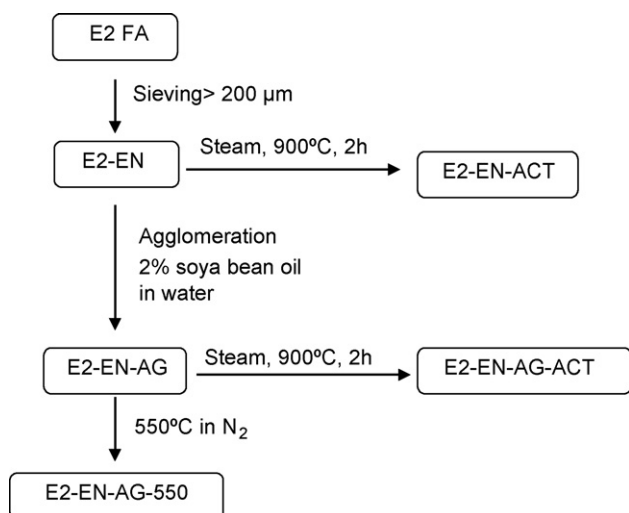
Fig. 1 shows a description of the history of the samples studied in this paper.

2.2. Samples characterization

The major and minor elements composition was obtained for the carbon-enriched samples by inductively coupled plasma (ICP Jobin-Yvon 2000), on a dissolution coming from acid digestion using LiB_4 and further HCl attack.

Powder X-ray diffraction (XRD) was used for phase mineral characterization. XRD profiles were obtained using Cu Kα radiation, range 2θ from 3° to 80°, step 0.05° and step time 5 s. In order to compare fractions, the X-axis is presented from 20° to 40°. The diffractograms were recorded in a DS-8 Advance instrument from Brucker.

Ultimate analyses were performed for C, H, N, O and S in a Thermo Flash 1112 analyzer.

Adsorption isotherms were performed in an Autosorb-1 from Quantachrome. Prior to the analysis, samples were outgassed at 250 °C under vacuum up to 10^{-5} mm Hg.

Mercury porosimetry analyses were carried out in a Pore-master from Quantachrome.

The morphological examination of the samples (coated with a gold layer) was done by means of SEM in a Hitachi S-3400N at several magnifications. In some cases secondary electrons images were obtained of samples embedded in a polished cross-section resin.

2.3. SO_2 adsorption experiments

An experimental installation built up for this purpose was used to test SO_2 removal capacity of samples. A diagram of the installation is shown in Fig. 2. A flow of 25 cc/min of gas containing 1000 ppmv SO_2, 5% (v/v) O_2, 6% (v/v) water vapor and Ar as balance was passed trough a bed of 2 g of sample at 100 °C of temperature. The concentration of each gas was
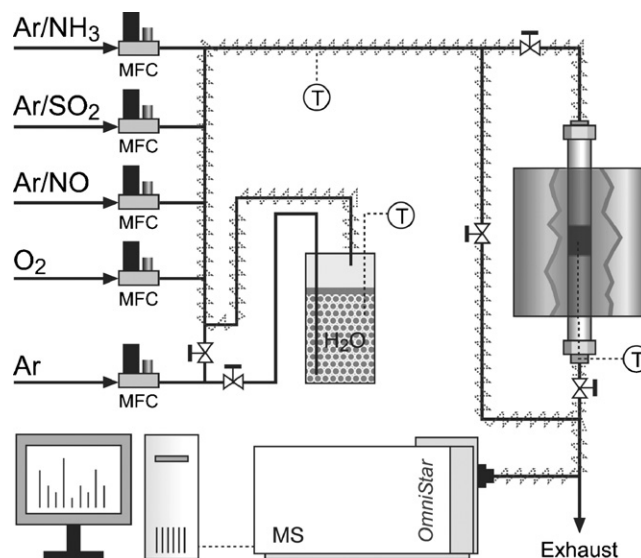

Fig. 1. Samples preparation.

Fig. 2. Experimental installation for SO_2 experiments (MFC: mass flow controller; MS: mass spectrometer; T: temperature controller).

Table 1
Elemental analysis of the studied fractions

	% weight (moisture free)				% ash (w/w)
	C	H	N	S	
E2-EN	12.35	0.01	0.15	0.34	84.9
E2-EN-ACT	6.05	0.07	0.00	0.05	92.8
E2-EN-AG	64.08	0.46	0.76	0.39	30.3
E2-EN-AG-550	60.25	0.38	1.07	0.32	33.6
E2-EN-AG-ACT	57.62	0.21	0.71	0.12	38.5

Table 3
Textural characterization by N_2 adsorption (surface area and total pore volume) and mercury porosimetry (intrusion volume and porosity)

	S_{BET} (m^2/g)	$V_{p/p_0} = 0.99$ (cm^3/g)	V_{int} (cm^3)	Porosity (%)
E2-EN	13	0.026	0.11	39.9
E2-EN-ACT	65	0.065	0.14	39.4
E2-EN-AG	2	0.014	0.17	35.2
E2-EN-AG-550	117	0.088	0.18	44.2
E2-EN-AG-ACT	416	0.297	0.31	46.6

measured by mass spectrometry. The presence of SO_3 in the outlet gases was also monitored.

The reaction results are described is terms of SO_2 adsorption: C/C_0, being C the concentration of SO_2 at a time t and C_0 the initial concentration of SO_2, measured when the gas stream is bypassed the reactor, before starting an experiment.

Regeneration of exhausted samples was carried out at 400 °C of temperature and a flow of 25 ml/min of Ar. The time in each regeneration experiment was variable, considering the final point when the concentration of SO_2 in the gas was below 50 ppmv.

3. Results and discussion

3.1. Characterization

Elemental analysis and ash content of the samples studied in this paper are given in Table 1. Hydrogen content is very low, indicating a high degree of condensation. Sample E2-EN-AG exhibit higher hydrogen content than expected and this fact can be attributed to remaining oil from agglomeration procedure in the sample.

The composition of ash of each sample, expressed as main oxides of metals, is shown in Table 2. It can be seen a high Fe content because the coal burned was a blend containing lignite with a high pyrite content. Main differences in ash composition after agglomeration process are observed in Ca and Fe compounds.

BET surface areas obtained from N_2 isotherms are reported in Table 3. The reported values are not corrected for their mineral matter content. The inorganic fraction made a relatively constant contribution to surface area values of roughly 0.7–0.8 m^2/g in any ash [13]. However, values of surface area in Table 3 were not corrected for the inorganic contribution because the samples are further used as they have been obtained and characterized and this type of correction would not reflect the real properties of the whole material.
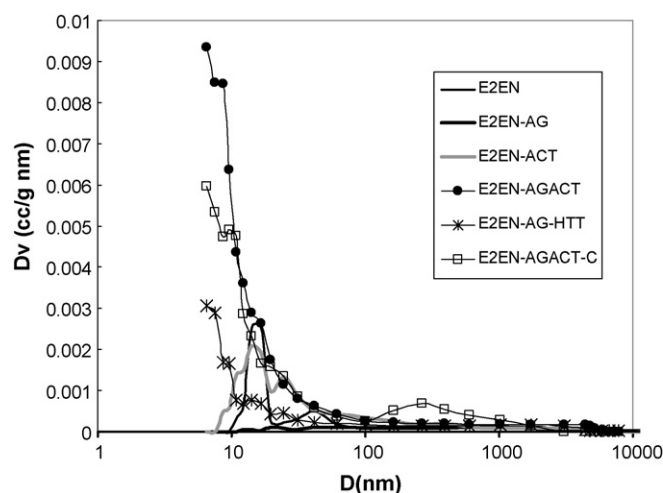

Fig. 3. Pore volume distribution as a function of the pore diameter.

Sample E2-EN-AG has a lower value of BET surface area than expected. This fact can be attributed to remaining oil that can be blocking pore entrances to adsorption gas [11]. After heating at 550 °C, a noticeable increase in BET surface area and in porosity of this sample can be observed. The surface area value of the activated sample (E2-EN-AG-ACT) is noteworthy, despite of their high ash content. Total pore volume follows the same trend that surface area. This is an important fact, because enough pore volume is needed for the storage of sulfuric acid obtained as a reaction product. The sample E2-EN-ACT has a lower BET surface area than the sample E2-EN-AG-ACT because of their very low carbon content (6.05%, see Table 1).

Intraparticle volume as well as porosity values obtained from mercury porosimetry are given in Table 3. Sample E2-EN-AG-ACT has the highest porosity, corresponding to the activation process undergone by the sample. On the other hand, sample E2-EN-AG exhibit the lowest porosity, indicating a pore blockage

Table 2
Ash composition of samples, expressed as a main metal oxides (%), obtained by ICP

	% M_xO_y							
	SiO_2	Al_2O_3	CaO	Fe_2O_3	K_2O	MgO	Na_2O	TiO_2
E2-EN	49.56	27.47	4.80	13.20	1.76	1.24	0.19	0.85
E2-EN-ACT	50.46	27.09	4.06	12.04	1.65	1.11	0.17	0.94
E2-EN-AG	50.86	31.22	3.66	7.09	1.15	1.17	0.20	1.10
E2-EN-AG-550	nd	nd	nd	nd	nd	nd	nd	nd
E2-EN-AG-ACT	50.45	34.76	2.66	4.80	0.99	1.04	0.14	1.31

due to remaining oil from agglomeration process. After heating at 550 °C in inert atmosphere, this sample exhibit, as expected, higher BET surface are and pore volume.

In Fig. 3 the pore volume distribution of the studied samples, obtained from mercury porosimetry, is shown. A very important increase in small mesopores volume (<12 nm) can be observed for the activated sample E2-EN-AG-ACT.

SEM microphotographs are depicted in Fig. 4. Images (a) correspond to secondary electrons and images (b) to backscattered electrons.
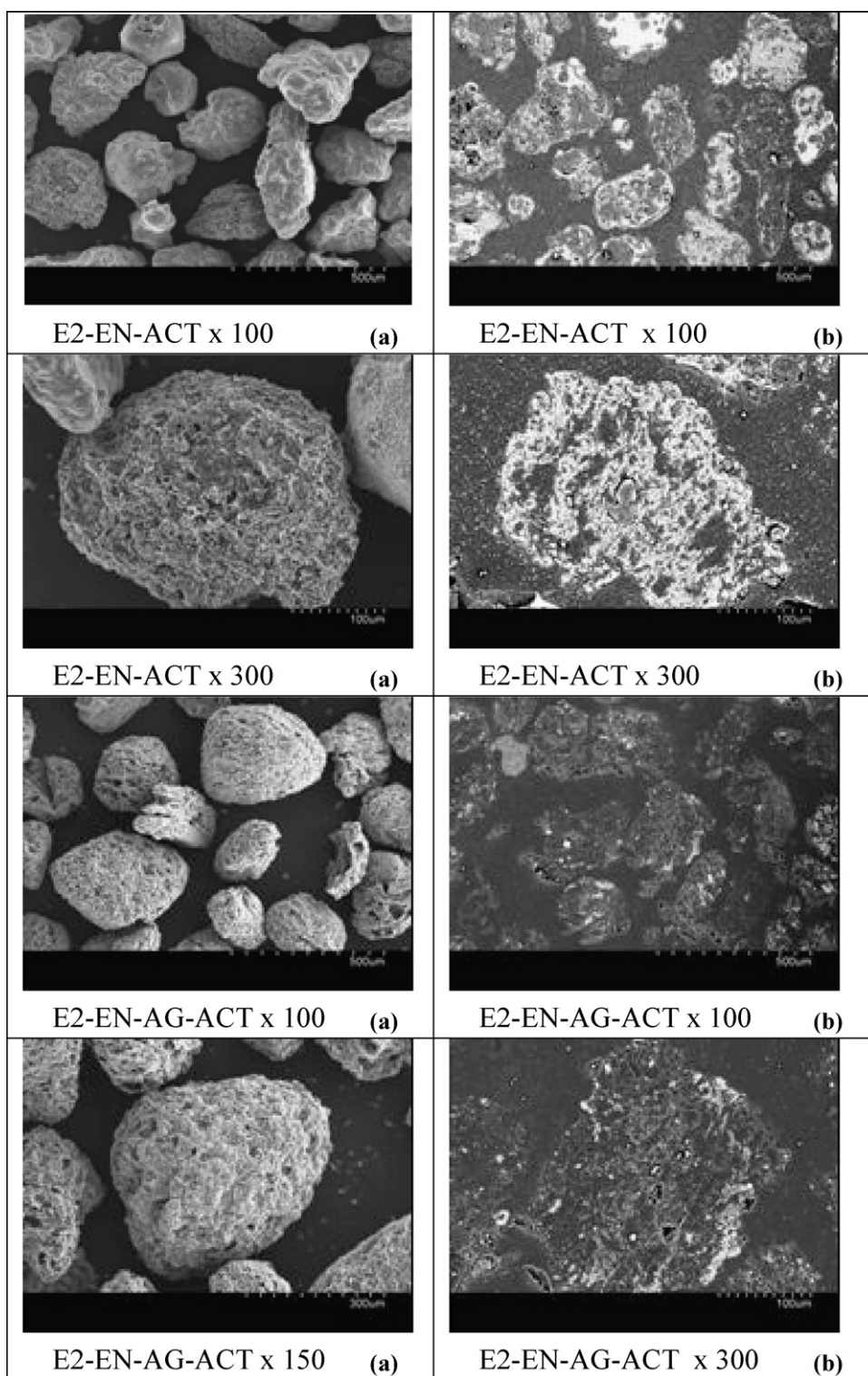

Fig. 4. SEM microphotographs of samples. (a) Images obtained with secondary electrons and samples dispersed as powder and (b) images obtained from back-scattered electrons and samples embedded in a polished resin.

Microphotographs of sample E2-EN-ACT obtained at magnification 100× show particles of mineral matter with an advanced fusion stage due to high temperatures reached during combustion. This type of particles cannot be observed in sample after agglomeration process E2-EN-AG-ACT.

At higher magnification, small differences in the morphology of particles coming from sieving-enriched sample or agglomerated one are found, despite of the content of carbon for both samples are quite different. However, comparing images obtained from powdered samples and those embedded in a polished resin (using backscattered electrons detector) differences are evident. Dark areas are composed of carbon structures, whereas higher intensity zones correspond to inorganic matter. From these images it can be concluded that agglomeration process has selected carbonaceous particles with less amount of mineral matter in the outer part of the particle, discarding particles mainly composed of inorganic matter. However, inorganic matter occluded inside carbon structures cannot be removed by this physical treatment.

3.2. SO₂ removal tests

The SO_2 breakthrough curves for samples E2-EN, E2-EN-AG, E2-EN-ACT and E2-EN-AG-ACT are depicted in Fig. 5. Experiments were carried out at 100 °C of temperature, total flow of 25 ml/min and a gas composition 1000 ppmv of SO_2, 5% (v/v) O_2, 6% (v/v) H_2O (Ar as balance). During the experiments, the evolution of SO_2, SO_3, O_2, H_2O were followed on-line.

Low SO_2 removal capacities are found for samples E2-EN, E2-EN-AG and E2-EN-ACT. Breakthrough occurs in few minutes, indicating that adsorption capacity is very low because of the poor developed porous system, according to data reported in Table 3. No evolution of SO_3 was observed during the experiments, indicating SO_2 adsorption without catalytic oxidation to SO_3, or SO_2 conversion to SO_3 followed to conversion to H_2SO_4. After some SO_2 removal tests, desorption experiments

Table 4
Amount of SO₂ removed by the studied samples at 50% breakthrough

Sample	SO₂ removed (mg)
E2-EN	0.15
E2-EN-ACT	0.66
E2-EN-AG	0.30
E2-EN-AG-550	1.30
E2-EN-AG-ACT	54.10

were carried out. During desorptions, no SO_3 was evolved and SO_2 was evolved at higher temperatures than those corresponding to physisorption. This fact could indicate that SO_2 is actually adsorbed and catalytically converted to H_2SO_4.

Breakthrough for sample E2-EN-AG-ACT occurs at 240 min. After this time a slow breakthrough process is observed, typical of granular activated carbons, because of wider pore size distribution compared to other carbons. Sulfuric acid is stored in appropriate pores, meaning that it has to move from bigger pores to pores in which potential is lower. This process can be controlled by diffusion problems if pore structure of carbons has not been well developed.

Table 4 reports the amount of SO_2 removed when breakthrough was 50%, from the experiments shown in Fig. 5. The 50% breakthrough point is achieved at different times for each sample, and big differences in removal capacity are found between the samples.
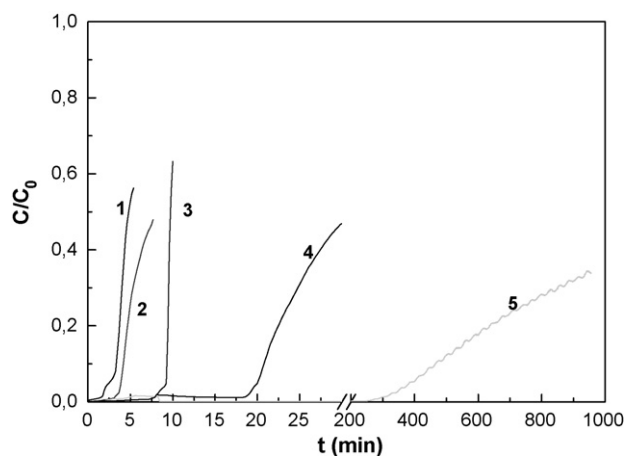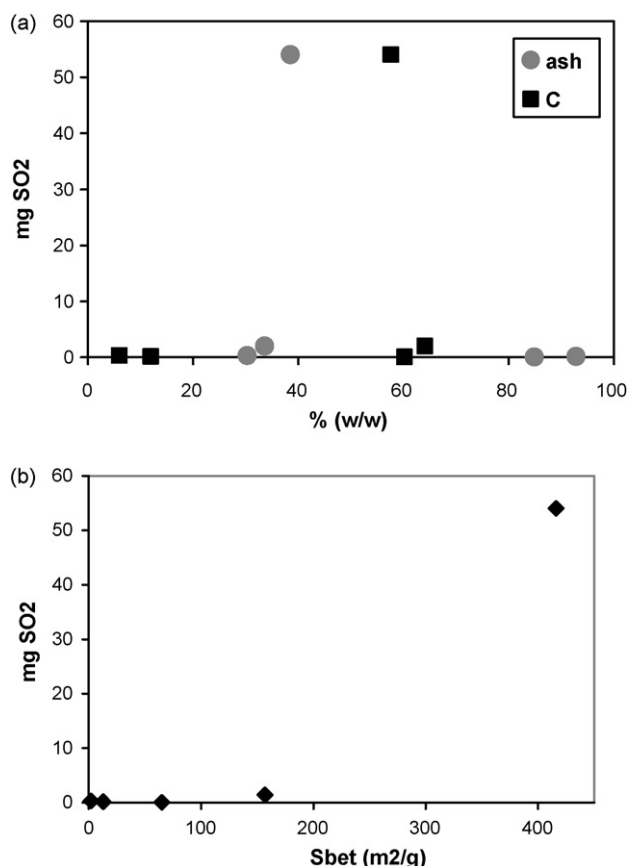

Fig. 5. SO₂ breakthrough curves of studied samples. Experimental conditions: temperature of reaction 100 °C, total flow 25 ml/min and gas composition 1000 ppmv of SO₂, 5% (v/v) O₂, 6% (v/v) H₂O and Ar as balance. (1) Sample E2-EN, (2) sample E2-EN-AG, (3) sample E2-EN-ACT (4) sample E2-EN-AG-550 and (5) sample E2-EN-AG-ACT.

Fig. 6. Relationship between SO₂ conversion and (a) ash and carbon content and (b) surface area.

Table 5
Elemental analysis and textural parameters of the sample E2-EN-AG-ACT after 5 cycles of SO$_2$ adsorption–desorption (E2-EN-AG-ACT-C)

	% weight (moisture free)				S_{BET} (m^2/g)	$V_{p/p_0} = 0.99$ (cm^3/g)	V_{int} (cm^3)	Porosity (%)
	C	H	N	S				
E2-EN-AG-ACT-C	49.7	0.17	0.57	0.40	309	0.226	0.19	46.0

It can be found in the literatures [14,15] work related with the influence on the SO$_2$ removal of ash content of active carbons. However, the differences observed in SO$_2$ removal capacity of the studied samples can be explained neither in terms of their total ash content nor in their ash composition. In Fig. 6a can be seen the lack of correspondence between the amount of SO$_2$ adsorbed and the ash and carbon content. In Fig. 6b the relationship between BET surface area and amount of SO$_2$ adsorbed is depicted. The highest amount of SO$_2$ removed corresponds to activated sample E2-EN-AG-ACT, which has the highest BET surface area. A similar trend can be observed with the other textural parameters obtained for this sample, pore volume and porosity (Table 3). The higher activity shown by the activated sample E2-EN-AG-ACT, therefore, can be attributed to their textural properties. However, the sample E2-EN-AG-550, which has a BET surface of 117 m^2/g, only removes 1.7 mg SO$_2$. Probably changes in surface chemistry during the activation process play also a role in the adsorption and catalytic conversion of SO$_2$ into H$_2$SO$_4$ [16–18].

The low activity shown by the other activated sample studied, E2-EN-ACT, can be attributed to its very low carbon content, 6.05%. As shown in previous works [9,16], carbon content and porosity are connected, because the activation only affects to carbonaceous part of the samples. Therefore, if the precursor has low carbon content, the obtained activated sample cannot show a high performance.

In the case of activated sample, cycles of SO$_2$ adsorption/regeneration were carried out in order to evaluate the possibility of thermal regeneration and re-use of these activated carbons. Regeneration of the exhausted carbons was carried out at 400 °C of temperature and a flow of 25 ml/min of Ar. Time used for regeneration was variable depending on the evolution of SO$_2$, considering the final point when the concentration was below 50 ppmv SO$_2$. Breakthrough curves after each desorption step are shown in Fig. 7.

During thermal regeneration of exhausted samples after their use in SO$_2$ abatement experiments the sulfuric acid stored on the carbon is removed acting the carbon as a reducer [10], following the reaction:

$$2H_2SO_4 + C \rightarrow 2SO_2 + CO_2 + 2H_2O$$

The gas evolved from this regeneration step is a SO$_2$-rich gas that can be further processed to produce elemental sulfur, liquid SO$_2$ or sulfuric acid.

Fig. 7 shows the SO$_2$ removal capacity of sample E2-EN-AG-ACT for six adsorption/regeneration cycles. As can be seen in this figure, after each cycle, the SO$_2$ removal capacity of the sample decreases, and the breakthrough starts earlier. Moreover, after each cycle the steepness of the breakthrough curves
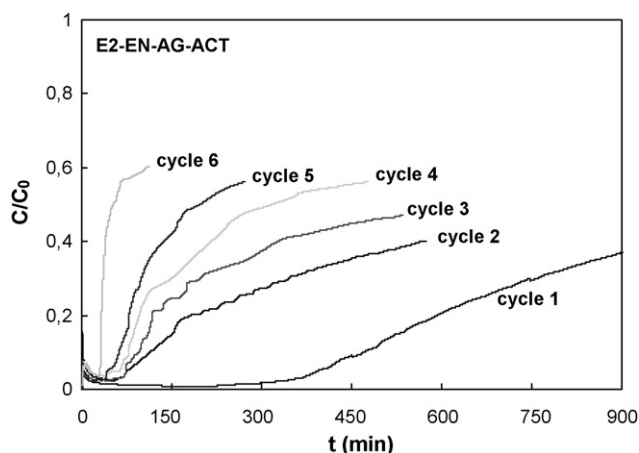

Fig. 7. Breakthrough curves after desorption step of sample E2-EN-AG-ACT. Experimental adsorption conditions: temperature of reaction 100 °C, total flow 25 ml/min and gas composition 1000 ppmv of SO$_2$, 5% (v/v) O$_2$, 6% (v/v) H$_2$O and Ar as balance. Desorption conditions: 400 °C of temperature and 25 ml/min Ar.

changes. This fact can be explained in terms of the reaction that put up with a mild gasification, leading to a pore opening. In Table 5, the elemental analysis as well as textural parameters of the sample E2-EN-AG-ACT regenerated after 5 cycles of SO$_2$ adsorption–desorption (named E2-EN-AG-ACT-C) are shown. A loss of BET surface area and total pore volume can be observed. Also, the carbon content has decreased (from 57.62% to 49.70%) because in each regeneration step, carbon is consumed. The pore size distribution of this sample obtained from mercury porosimetry (Fig. 3) show a noteworthy decrease of small mesopores, together with an increase in macropores. These changes in textural properties could be the main cause of the loss of SO$_2$ removal capacity of this sample. The behavior of this sample, however, differs from that observed by the authors in the same conditions for low temperature coal chars [19], which can be thermally regenerated without loss of activity.

Work is in progress in order to determine the influence of surface oxygenated groups on the SO$_2$ adsorption capacity of the activated samples as well as on their loss of capacity after thermal regeneration.

4. Conclusions

This work has shown that the carbon-enriched fraction present in FAs can be a precursor of activated carbons. After an agglomeration process these carbons only requires a process of activation since it has gone through a devolatilization during the combustion in the furnace of the power station. After activation, an activated carbon with medium surface area can be

obtained for environmental application. In the present case, SO_2 removal capacity has been tested onto these samples, obtained promising results.

References

[1] ECOBA, European association for use of the by-products of coal-fired power-stations, 2005, http://www.ecoba.com.

[2] K.A. Lindon, The Properties and Use of Coal Fly Ash, Thomas Telford Ltd., London, 2001.

[3] M.M. Maroto-Valer, D.N. Taulbee, H.H. Schobert, J.C. Hower, J.M. Andresen, Use of unburned carbon in fly ash as precursor for the development of activated carbons, in: International Ash Utilization Symposium. Paper#19, 1999.

[4] J.P. Baltrus, A.W. Wells, D.J. Fauth, J.R. Diehl, C.M. White, Characterization of carbon concentrates from coal combustion fly ash, Energy Fuels 15 (2001) 455–462.

[5] V.M. Graham, T.L. Robl, R.F. Rathbone, Adsorptive properties of FA Carbon, ACS Div. Fuel Chem. 43 (1996) 983–988.

[6] S. Wang, Y. Boyjoo, A. Choveib, E. Ng, H. Wu, Z. Zhu, Role of unburnt carbon in adsorption of dyes on FA, J. Chem. Technol. Biotechnol. 80 (2005) 1204–1209.

[7] M.M. Maroto-Valer, Y. Zhang, E.J. Granite, Z. Tang, H.W. Pennline, Effect of porous structure and surface functionality on the mercury capacity of a fly ash carbon and its activated samples, Fuel 84 (2005) 911–916.

[8] M.A. Lopez-Alonso, M. Diaz-Somoano, M.R. Martinez-Tarazona, Retention of elemental mercury on fly ashes in different atmospheres, Energy Fuels 21 (2007) 99–103.

[9] B. Rubio, M.T. Izquierdo, M.C. Mayoral, M.T. Bona, J.M. Andrés, Unburnt carbon from coal fly ashes as a precursor of activated carbon for nitric oxide removal, J. Hazard. Mater. 142 (2007) 561–566.

[10] E. Richter, Carbon catalysts for pollution control, Catal. Today 7 (1990) 93–112.

[11] B. Rubio, M.T. Izquierdo, M.C. Mayoral, M.T. Bona, R.M. Martinez-Tarazona, Preparation and characterization of carbon-enriched coal fly ash, J. Environ. Manage., doi:10.1016/j.jenvman.2007.07.027.

[12] M.I. Alonso, A.F. Valdes, R.M. Martinez-Tarazona, A.B. Garcia, Coal recovery from coal fines clearing wastes by agglomeration with vegetable oils: effects of oil type and concentration, Fuel 78 (1999) 753–759.

[13] I. Külaots, R.H. Hurt, E.M. Suuberg, Size distribution of unburned carbon in coal fly ash and its implication, Fuel 83 (2004) 223–230.

[14] P. Davini, Adsorption and desorption of sulphur dioxide from simulated gas on active carbon: the effect of the ash content, Carbon 31 (1993) 47–51.

[15] P. Davini, The effect of certain metallic derivatives on the adsorption of sulphur oxide on active carbon, Carbon 39 (2001) 419–424.

[16] B. Rubio, M.T. Izquierdo, A.M. Mastral, Influence of low-rank coal char properties on their SO_2 removal capacity from flue gases. 2. Activated chars, Carbon 36 (1998) 263–268.

[17] A.A. Lizzio, J.A. DeBarr, Mechanism of SO_2 removal by carbon, Energy Fuels 11 (1997) 284–290.

[18] K. Li, L. Ling, C. Lu, Z. Liu, L. Liu, I. Mochida, Influence of CO-evolving groups on the activity of activated carbon fibre for SO_2 removal, Fuel Process. Technol. 70 (2001) 151–158.

[19] M.T. Izquierdo, B. Rubio, C. Mayoral, J.M. Andres, Low cost coal-based carbons for combined SO_2 and NO removal from exhaust gas, Fuel 82 (2003) 147–151.